Hindawi
Shock and Vibration
Volume 2021, Article ID 5538179, 11 pages
https://doi.org/10.1155/2021/5538179

Research Article

Rock Burst Mechanism under Coupling Action of Working Face Square and Regional Tectonic Stress

Sitao Zhu,[1] **Decheng Ge**,[1] **Fuxing Jiang**,[1] **Cunwen Wang**,[2] **Dong Li**,[3] **Xiaoguang Shang**,[1] **Baoliang Zhang**,[4] **and Zhaoyi Wang**[5]

[1]*School of Civil and Resource Engineering, University of Science and Technology Beijing, Beijing 100083, China*
[2]*Research Center for Rock Burst Control of Shandong Energy Group Co., LTD, Jinan 250014, Shandong, China*
[3]*Safety Engineering College, North China Institute of Science and Technology, Beijing 101601, China*
[4]*School of Architecture & Civil Engineering, Liaocheng University, Liaocheng 252059, Shandong, China*
[5]*Liangbaosi Coal Mine, Shandong Energy Feicheng Mining Group Co., LTD, Jining 272400, Shandong, China*

Correspondence should be addressed to Decheng Ge; b20180034@xs.ustb.edu.cn

Received 2 February 2021; Revised 3 March 2021; Accepted 15 April 2021; Published 3 May 2021

Academic Editor: M.I. Herreros

With the development of faults in many coalfields, many large faults will form a relatively independent area, forming regional tectonic stress concentration. Under the influence of mining, it is easy to induce fault activation, produce mine tremor, and then induce rock burst. Through field investigation, theoretical analysis, numerical simulation, and engineering verification, the overburden movement model of No. 3504 working face square and fault activation in Liangbaosi Coal Mine was established. The stress variation and energy release law of working face advance and fault area were analyzed, and the mechanism of rock burst under the coupling action of working face square and regional tectonic stress was revealed. The results show that the regional stress adjustment and fault activation are caused by the large-scale overall movement of overburden during the working face square, and there is a peak value of elastic energy release during the fault activation, which is easy to produce large energy mine earthquake. The energy level of the daily maximum energy event is higher than that of the initial mining stage in the square period, and the location of on-site large energy microseismic event is basically consistent with the predicted fault strike. The study provides a theoretical basis for the prevention and control of rock burst during the working face square under the condition of regional tectonic stress.

1. Introduction

The change of stress state in the fault area is the cause of rock burst and other dynamic disasters in many mines [1, 2]. For example, the 2305s fully mechanized top coal caving face in Xinjulong Coal Mine is obliquely intersected with FD8 fault (with a drop of 10–15 m), and serious rock burst accidents occurred in the upper roadway and combined roadway during the fault crossing, resulting in 4 deaths. The problem of rock burst near the fault structure has not been completely solved.

The predecessors have made fruitful achievements in the study of rock burst near fault structures. Li et al. [3] emphatically studied the disaster mechanism of fault dislocation type rock burst from four aspects: fault activation mechanism and its criterion, fault dislocation type rock burst theory, occurrence condition, and incubation process. Lyu et al. [4] studied the induction mechanism of reverse fault to rock burst from the aspects of in situ stress environment of reverse fault zone, stress characteristics of coal body near fault under the influence of mining, and dynamic load impact effect of fault activation instability sliding on the working face under the influence of mining. Zhang et al. [5] studied the unloading instability mechanism of thrust fault, including unloading instability mode, instability process, and energy transfer of instability transient. Lin et al. [6] studied the mechanical mechanism and stability control of fault self-locking and activation. Li et al. [7] studied the spatial evolution law of

mining stress and the risk of rock burst in the fault zone. Wang et al. [8] studied the stress field evolution characteristics of thrust fault sliding surface under mining disturbance. Jiang et al. [9, 10] studied the fault activation law under the influence of mining. Li et al. [11] studied the activation conditions of giant thrust faults under mining disturbance. Jiang et al. [12] studied the triggering mechanism of a tunnel surrounding rock fault sliding fracture under external disturbance. Xia et al. [13] studied the in situ stress criterion of fault activation. Zhu et al. [14] studied the fault activation law of a fully mechanized top coal caving face in a deep and extra thick coal seam. Jiang et al. [15, 16] studied the evolution of mining stress and the characteristics of fault activation under hard and thick strata. Zhao et al. [17] considered that the dynamic evolution of mining pressure relief area, support pressure boosting area, and original stress area formed by the surrounding rock of the working face from inside to outside will induce fault structure dislocation activation. Jiao et al. [18] studied the dynamic mechanical response characteristics of faults under mining disturbance and analyzed the mutual feedback mechanism between stope strata behavior and fault damage slip. Li et al. [19] studied the influence of different dip angles of reverse faults on stope rock burst. Lu et al. [20] studied the precursory law of rock burst induced by fault sliding. Zhu et al. [21] studied the rock burst mechanism of fault slip and instability when mining in isolated working faces near faults. Zhao et al. [22] studied the characteristics of a regional in situ stress field under the influence of multistage tectonic movement and its influence on rock burst. Li et al. [23] analyzed the in situ stress field distribution characteristics of three gold mines with frequent microseismic activities. Zhang et al. [24] studied the variation law of surrounding rock stress after excavation. Lyu et al. [25] studied the fault activation law and induced rock burst mechanism of the deep working face. Zhang [26] studied the rock burst mechanism of mining roadway under the coupling condition of structure and thick conglomerate. Wang et al. [27] studied the temporal and spatial evolution characteristics of fault structure dislocation and slip and statistically analyzed the evolution law of actual mine earthquake source activity in a mining face. Wang et al. [28] believe that the mechanism of rock burst induced by fault structure is the superposition of tectonic stress and mining stress. Zhu et al. [29] studied the relationship between active faults and rock burst risk. Jiang et al. [30] adopted "the three-zone loading" theoretical model superimposed with tectonic stress to realize the approximate calculation of external stress and then obtained the rock burst risk of surrounding rock. Wang et al. [31] studied the movement process of overlying strata, abutment pressure of working face dip, and stress variation law of fault plane in footwall coal seam mining of giant thrust fault. Wang et al. [32] considered that the masonry beam structure is more likely to be formed after the key layer is broken in the hanging wall mining, the stability of the structural system is higher than that in the footwall mining, and the rock burst hazard of the working face is higher in the footwall mining. Zhang et al. [33] considered that the great release of strain energy stored in the surrounding rock led to rock burst. Tarasov and Randolph [34] considered that the energy released by deep earthquakes and rock bursts is extremely high due to a very low shear resistance structure formed in the process of fault development. Jiang et al. [35] studied the classification and early warning method of tectonic controlled rock burst by using the microseismic monitoring method. Meng et al. [36] proposed the prediction method of stress drop based on acoustic emission b value and the prediction method of fault sliding rock burst caused by stress drop. Jiang et al. [37] studied the dynamic analysis method of rock burst risk of a longwall working face intersecting with fault. Cong et al. [38, 39] evaluated the increase of rock burst risk caused by dynamic load disturbance in the fault area through the vibration effect index. Li et al. [40] studied the disaster mechanism and safe mining technology when the working face of deep well, thick topsoil, and thick bedrock is mined to the square position. Jiang et al. [41, 42] studied the overburden spatial structure before and after the square and the calculation of working face stress. Wang et al. [43] studied that there are initial influence range, significant influence range, and severe influence range in the square stage of working face. Kong et al. [44] studied the mechanism of abnormal weighting at the square position of the longwall working face. However, the rock burst mechanism under the coupling effect of working face square and regional tectonic stress is not deep enough.

Based on the engineering background of faults encountered in No. 3504 working face of Liangbaosi Coal Mine in Juye Coalfield, the stress variation law under the coupling condition of working face square and fault structure was studied, which revealed that the large-scale movement of overburden during working face square caused the regional stress adjustment of the fault structure. The mine earthquake caused by fault activation is the power source of local roadway impact failure.

2. Project Overview

2.1. Overview of Working Face. Liangbaosi Coal Mine is located in the southwest of Shandong Province, China. No. 3504 working face is located in the south of 3500 mining area, the working face elevation is −812.1~−985.7 m, and the ground elevation is +36.4~+39.2 m. The thickness of coal seam is 4.6~7.4 m, with an average of 6.5 m. The fully mechanized top coal caving technology is adopted. The strike length of the working face is 2793 m, the dip length is 96 m, and the area is 268128 m^2. As of May 1, 2020, 103 m of coal mining has been pushed in No. 3504 working face.

The south of the working face is close to the footwall waterproof coal pillar of F7 fault, and the east is close to F42 fault. No. f174 fault is developed in the face, as shown in Figure 1, and the fault parameters are shown in Table 1. The nearest distance between the working face and the goaf of No. 35001 working face (stopping time around April 2015) is 223 m.

2.2. Roof and Floor of Coal Seam. The comprehensive columnar condition of the coal seam in the working face is shown in Table 2. According to the comprehensive columnar analysis of the coal seam in the working face, there are 2.5 m

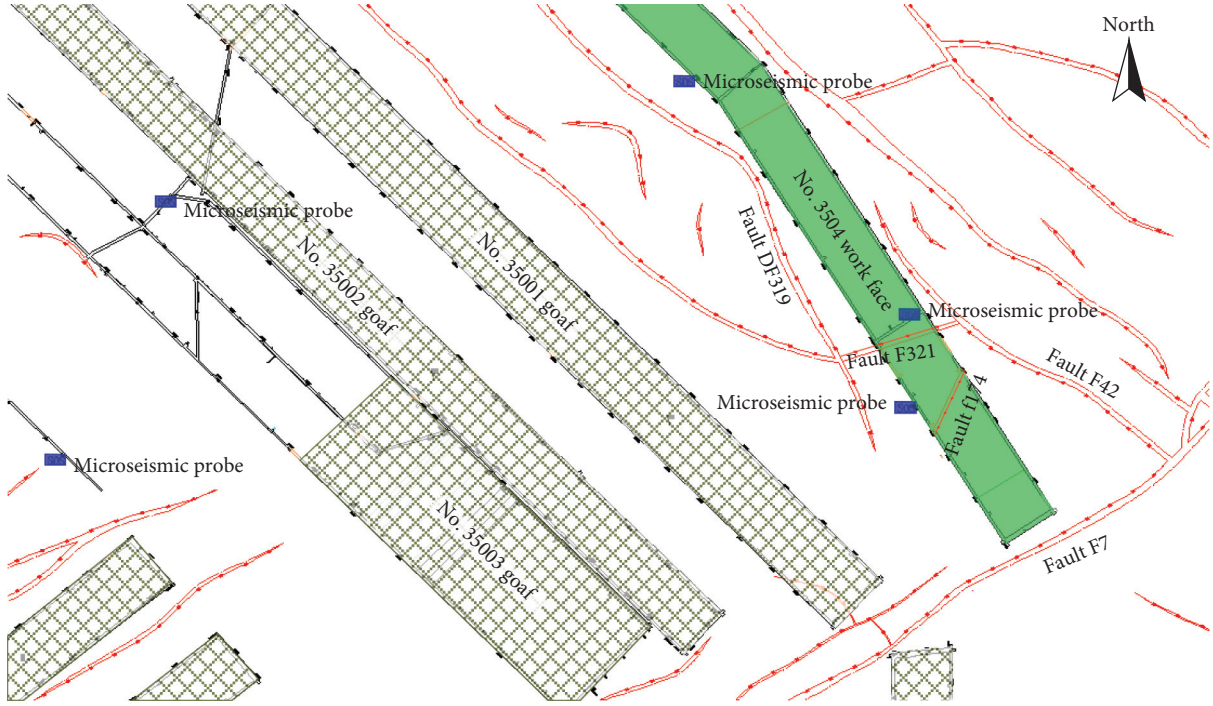

Figure 1: Relative position of working face.

siltstone, 5.5 m fine sandstone, 8.9 m siltstone, and 1.6 m medium sandstone above the coal seam in the working face, with a total of 18.5 m hard rock stratum. Then there is a 14.8 m thick sandstone group separated by 4.2 m mudstone above, and there is a 11.3 m thick medium sandstone layer upward.

2.3. Monitoring Method of Working Face. SOS microseismic monitoring system is installed in the mine. Five SOS microseismic probes are arranged near the working face, as shown in Figure 1.

KJ550 stress online monitoring system is installed in the working face to monitor the coal stress in real time. 12 groups (48 measuring points) are arranged according to the spacing of 25 m within 300 m ahead of the two crossheadings of the working face.

The two crossheadings of the working face are managed according to the strong rock burst hazard area, and the two crossheadings of the working face are monitored by drilling cuttings every day according to the spacing of 30 m, 60 m, and 90 m.

2.4. Roadway Rock Burst. At 3:00 on May 2, 2020, SOS microseismic system received a microseismic event with an energy of 2.15×10^5 J, and a coal cannon was heard at the scene. The incident was located 54.4 m in front of No. 3504 working face, near the rail alignment. There is no broken bolt or anchor cable in the site, and the roadway support is in good condition without obvious deformation. The floor heave of 42–48 m ahead of the track trough is about 8 cm, and 8 single pillars are drilled into the floor, as shown in Figure 2.

3. Coupling Mechanism of Working Face Square and Regional Tectonic Stress

3.1. Large-Scale Movement of Overburden Caused by Working Face Square. The mining area of the working face is about 890 m deep, and the gravity stress is high. In the process of mining, there is a low stress early warning at the stress online monitoring point, which indicates that the local stress concentration is caused in the mining process. The working face has been mined to 103 m, which is in the square stage of working face, and the roof moves in a large range. As shown in Figure 3, when the working face is mined to the square position, the height of overburden fracture reaches the maximum, and the overburden space movement is the most intense.

3.2. Fault Activation Caused by Regional Stress Adjustment. The whole movement of rock structure formed between the goaf and the weak fault plane of the working face is easy to cause the fault activation and form the mine earthquake, as shown in Figure 4.

4. Numerical Simulation of Coupling Action between Working Face Square and Regional Tectonic Stress

4.1. Modeling. The strain softening model was established by FLAC^{3D} software, with length × width × height = 529 m × 200 m × 160 m, as shown in Figure 5. The bottom and lateral boundaries were fixed, and 20.15 MPa was applied at the top of the model to replace the 806 m strata. The fault is normal fault with dip angle of 60°.

Table 1: Fault parameters.

Number	Property	Dip angle (°)	Fall (m)
f174	Normal fault	60	4
F321	Normal fault	50	16
F7	Normal fault	70	10–30
F42	Normal fault	70	30
F319	Normal fault	60–70	0–10

Table 2: Thickness of coal and rock strata.

Number	Lithology	Thickness (m)	Accumulated thickness of roof (m)
1	Medium sandstone	4.2	93.7
2	Siltstone	6.9	89.5
3	Medium sandstone	3.7	82.6
4	Siltstone	3.1	78.9
5	Mudstone	6.5	75.8
6	Medium sandstone	11.3	69.3
7	Siltstone	7.4	58
8	Mudstone	8.2	50.6
9	Siltstone	5.3	42.4
10	Medium sandstone	9.5	37.1
11	Sandstone	4.9	27.6
12	Mudstone	4.2	22.7
13	Medium sandstone	1.6	18.5
14	Siltstone	8.9	16.9
15	Fine sandstone	5.5	8
16	Siltstone	2.5	2.5
17	Coal	6.5	—
18	Siltstone	3.6	—
19	Fine sandstone	19	—

(a) (b)

Figure 2: Single pillars drilling into floor.

4.2. Stress Variation Law. Ten stress measuring points are, respectively, set in front of the middle of the working face and on the fault, and the positions of the measuring points are shown in Figure 6. The distance between the measuring points in front of the working face is 10 m, and the vertical distance between the fault measuring points is 6~12 m.

After the excavation of the working face, the change of vertical stress in the leading area of the working face is shown in Figure 7. The vertical stress has an obvious stress increasing stage, which is caused by the square of working face.

The change of horizontal stress in advance area of working face is shown in Figure 8. After the excavation, the horizontal stress changes obviously.

The vertical stress variation of fault measuring points is shown in Figure 9. The vertical stress has an obvious stress fluctuation stage, which is a fault activation process.

The change of horizontal stress at fault measuring points is shown in Figure 10. There is an obvious fluctuation stage of horizontal stress, the stress in some areas increases, and the stress in some areas decreases.

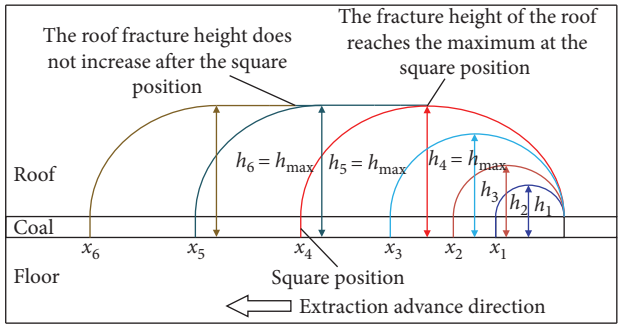

Figure 3: Height of fractured zone in overlying strata. x_i is the mining position of working face. h_i is the height of overburden fracture when mining face reaches x_i.

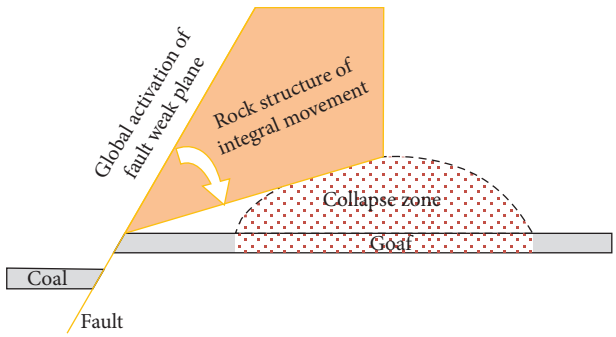

Figure 4: Schematic diagram of fault activation.

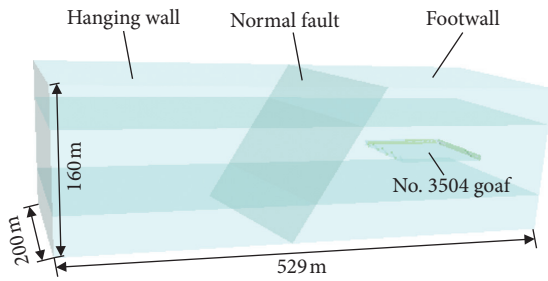

Figure 5: Schematic diagram of numerical model.

4.3. Energy Variation Law of Fault Area. The method described in [45, 46] is used to compile FISH language to monitor the elastic energy of each unit and accumulate the elastic energy released in the fault area. The variation law is shown in Figure 11. The peak value in the figure is the maximum value of concentrated release of elastic energy, which is the maximum energy burst instantly when the fault is activated during the stress adjustment stage.

5. Engineering Verification

5.1. Microseismic Monitoring. From February 28, 2020, to May 2, 2020, 4 large energy events occurred, respectively, on March 6, March 17, April 12, and May 2. The maximum energy values of a single event are 5.86×10^4 J, 8.41×10^4 J, 3.37×10^4 J, and 21.5×10^4 J, respectively, showing a

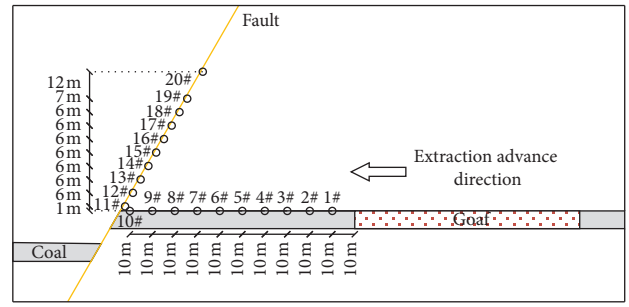

Figure 6: Layout of stress measuring points.

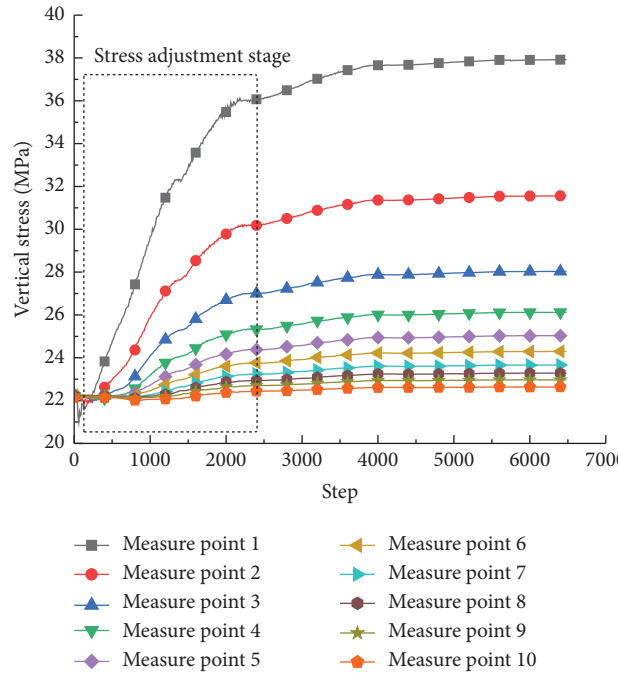

Figure 7: Vertical stress in leading area of working face.

gradually increasing trend, as shown in Figure 12. The location of each event is shown in Figure 13. On May 2, when the working face was pushed to square position, the energy of microseismic event was the largest, which also showed that the whole movement of overburden was the most intense and the energy released was the largest.

5.2. Cuttings Test. After the high energy event occurred on May 2, 6 drilling holes were constructed within 40 m before and after the track trough source. The amount of drilling cuttings is the largest at 11 m of one drilling cuttings hole 82 m ahead of the track, with a value of 6.1 kg/m, showing a yellow warning, and rock can be seen here. The amount of drilling cuttings of the other five drilling holes is normal, as shown in Figure 14.

According to the rock penetration of drilling cuttings hole, it is estimated that there are unproved faults along the outer side of the track. The working face is in the island-like area surrounded by faults F7, F42, f174, and DF319, and the regional tectonic stress is concentrated, as

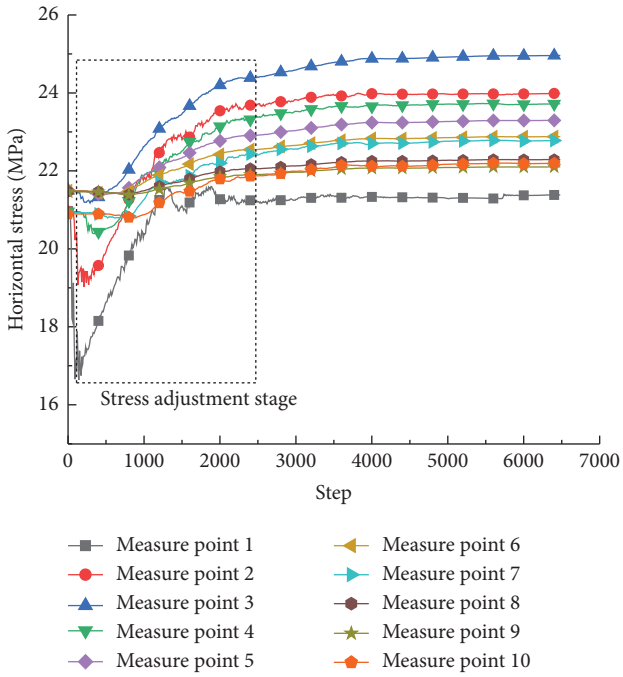

Figure 8: Horizontal stress in leading area of working face.

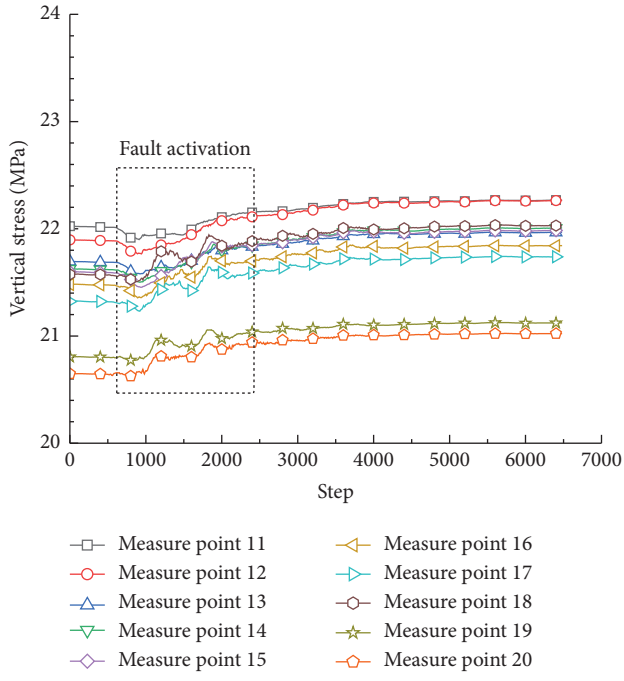

Figure 9: Vertical stress of fault measuring points.

shown in Figure 15. Through the location of 4 large energy microseismic events, we can see that the location of large energy microseismic events is consistent with the predicted fault.

5.3. KJ550 Stress Online Monitoring System. During the period from April 26 to May 1, the stress of 4# deep hole measuring points along the track increased by more than 1 MPa for many times, reaching the low stress warning; and

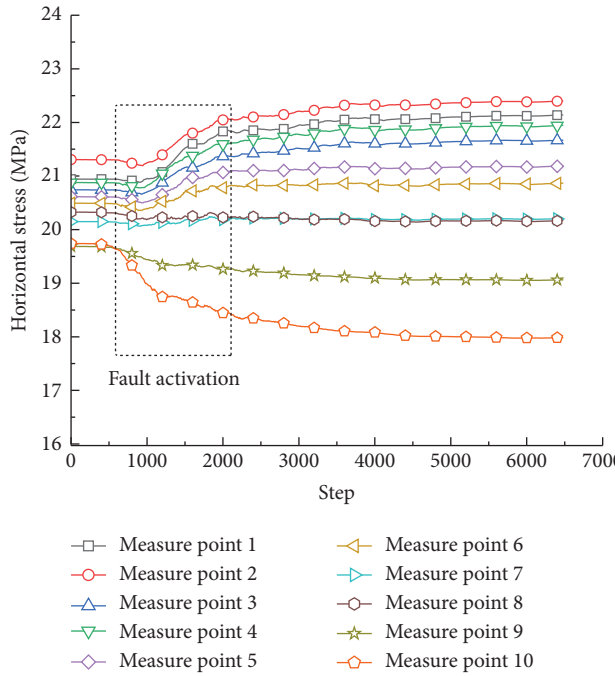

Figure 10: Horizontal stress of fault measuring points.

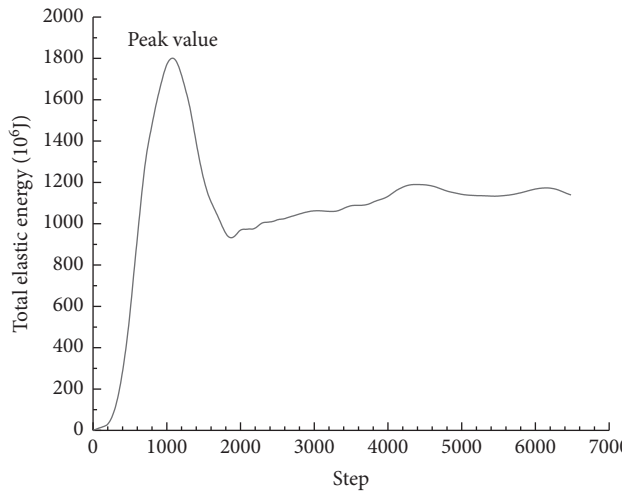

Figure 11: Variation of elastic energy in fault area.

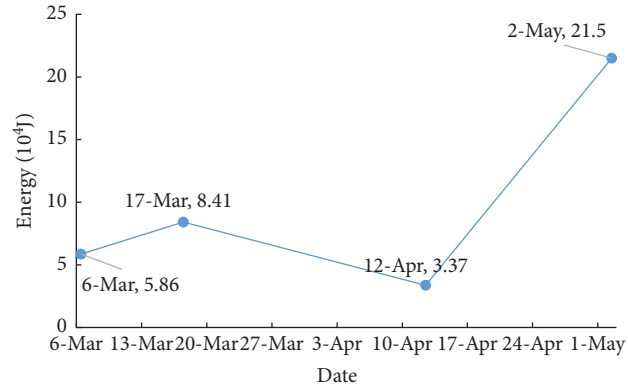

Figure 12: Energy statistical chart of 4 large energy microseismic events.

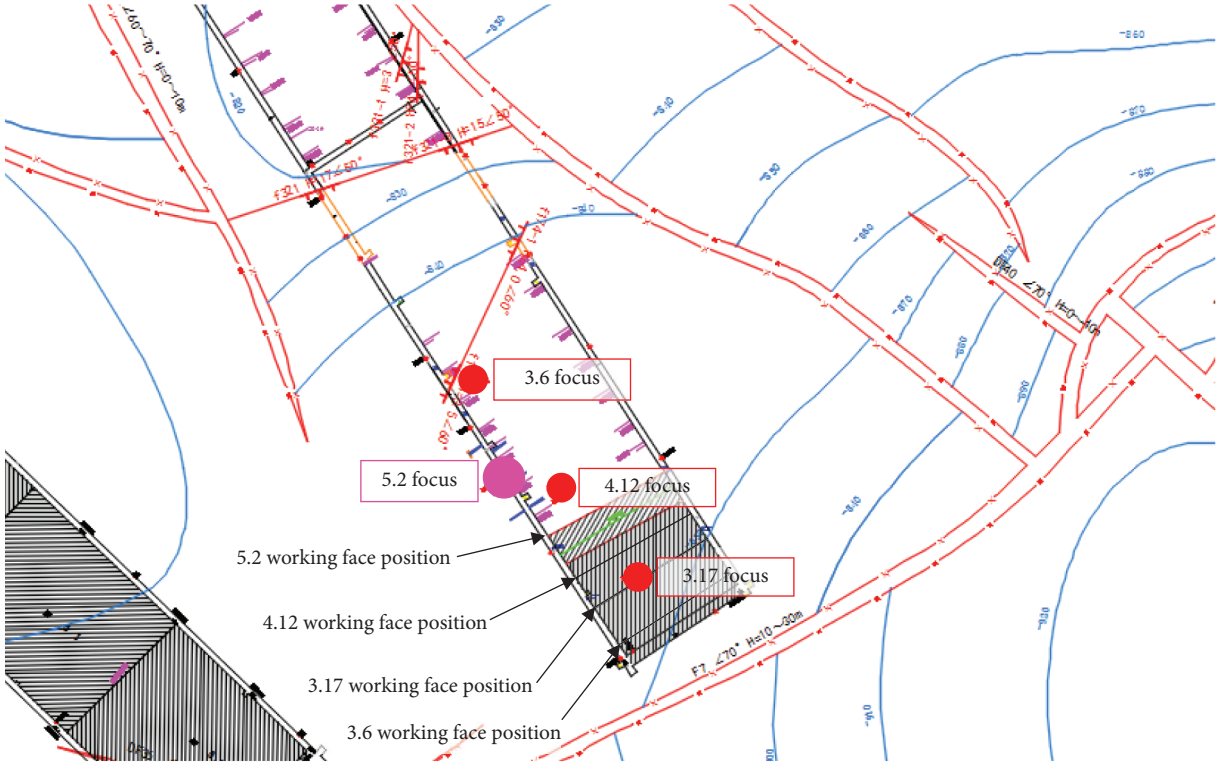

Figure 13: Location of four large energy microseismic events.

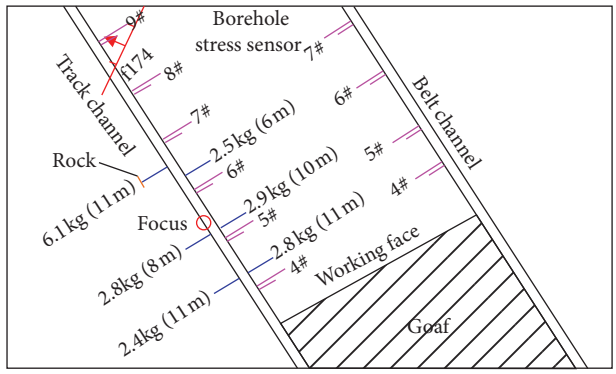

Figure 14: Cuttings inspection chart.

there is an instantaneous increase of more than 1 MPa. From 03:00 on May 1 to 02:14 on May 2, it increased from 5.41 MPa to 6.05 MPa, with an increase of 0.64 MPa, as shown in Figure 16.

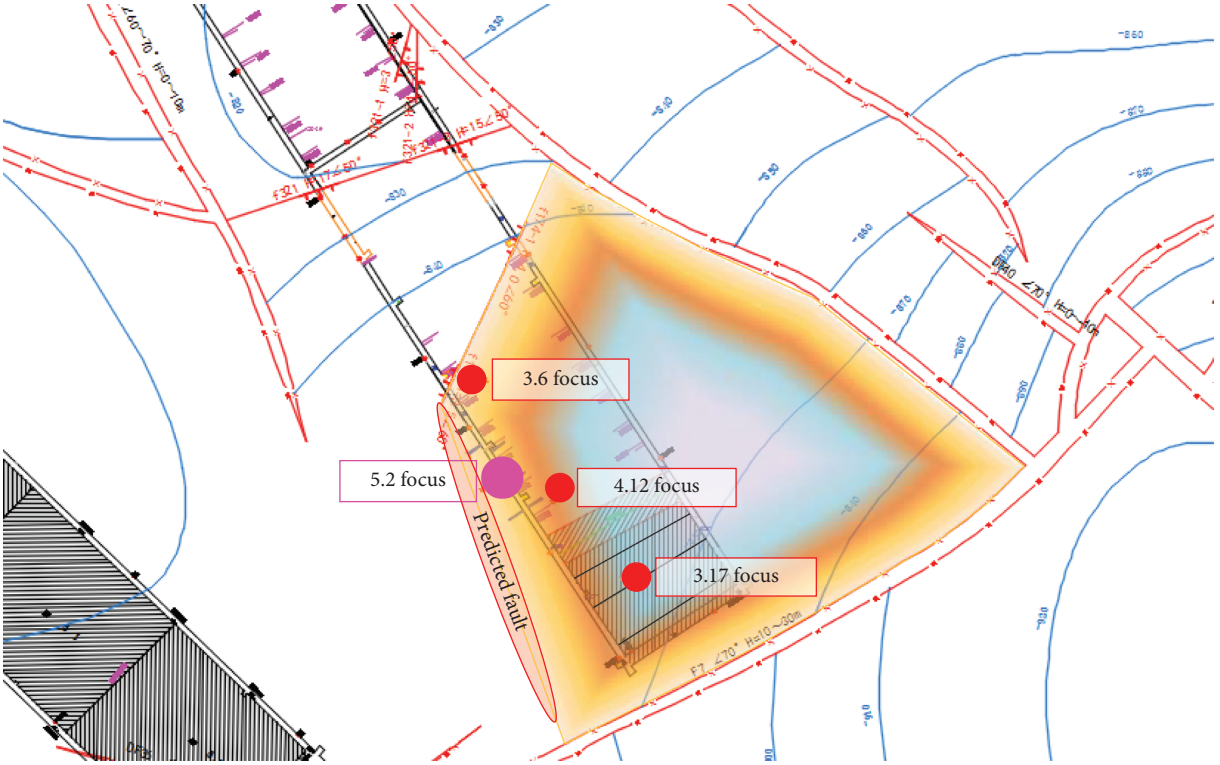

Figure 15: Schematic diagram of regional tectonic influence.

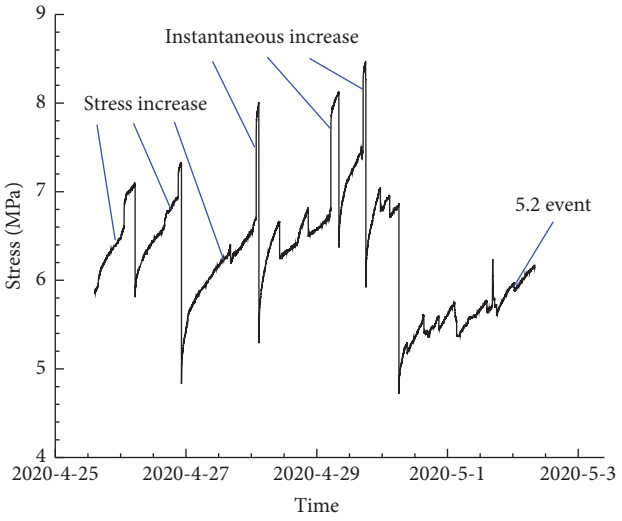

Figure 16: Borehole stress curve.

6. Conclusions

The mechanism of rock burst under the coupling action of square and regional tectonic stress in No. 3504 working face of Liangbaosi Coal Mine was studied; and the main conclusions are as follows:

(1) When the working face reaches square position, the overlying rock moves in a large range, and the leading position of the working face and the stress adjustment of the fault face lead to the activation of the fault, which is prone to large energy mine earthquake.

(2) In the initial mining stage, No. 3504 working face is located in the island-like area surrounded by F7 fault, F42 fault, and f174 fault, and the tectonic stress is concentrated in the area.

(3) Under the coupling effect of mining influence of working face square and regional tectonic stress

concentration, a large energy mine earthquake is produced. After the energy is transferred to the roadway, it leads to the rock burst of the roadway.

Data Availability

The data used to support the findings of this study are available from the corresponding author upon request.

Conflicts of Interest

The authors declare that there are no conflicts of interest regarding the publication of this paper.

Acknowledgments

The authors would like to thank all members in Shandong Energy Group Co., LTD., for their help with the fieldwork. This research was supported by the National Natural Science Foundation of China (Grants nos. 51634001 and 51904017), Major Scientific and Technological Innovation Projects in Shandong Province (Grant no. 2019SDZY02), the Fundamental Research Funds for the Central Universities (Grant no. FRF-TP-20-002A2), project funded by China Postdoctoral Science Foundation (Grant no. 2020M682214), and the Scientific Research Fund of Liaocheng University (Grants nos. 318011901 and 318012014).

References

[1] B. Shen, Y. Duan, X. Luo et al., "Monitoring and modelling stress state near major geological structures in an underground coal mine for coal burst assessment," *International Journal of Rock Mechanics and Mining Sciences*, vol. 129, Article ID 104294, 2020.

[2] B. Zhang, H. Zhou, Q. Chang, X. Zhao, and Y. Sun, "The stability analysis of roadway near faults under complex high stress," *Advances in Civil Engineering*, vol. 2020, Article ID 8893842, 10 pages, 2020.

[3] P. Li, M. Cai, Q. Guo, X. Lu, and B. Yan, "Research situations and development tendencies of fault slip rockburst in coal mine," *Journal of Harbin Institute of Technology*, vol. 50, no. 3, pp. 1–17, 2018.

[4] J. Lyu, T. Wang, W. Ding, Y. Pan, and C. Nan, "Induction mechanisms of coal bumps caused by thrust faults during deep mining," *Journal of China Coal Society*, vol. 43, no. 2, pp. 405–416, 2018.

[5] N. Zhang, S. Zhao, Y. Zhao et al., "Mechanism of thrust fault rupture causing by unloading effect," *Journal of China Coal Society*, vol. 45, no. 5, pp. 1671–1680, 2020.

[6] Y. Lin, M. Tu, B. Fu, and C. Li, "Mechanical mechanisms of fault self-locking and activation and its stability control," *Journal of Mining & Safety Engineering*, vol. 36, no. 5, pp. 898–905, 2019.

[7] T. Li, Z. Mu, G. Liu, J. Du, and H. Lu, "Stress spatial evolution law and rockburst danger induced by coal mining in fault zone," *International Journal of Mining Science and Technology*, vol. 26, no. 3, pp. 409–415, 2016.

[8] H. Wang, M. Shao, G. Wang, and D. Deng, "Characteristics of stress evolution on the thrust fault plane during the coal mining," *Journal of China Coal Society*, vol. 44, no. 8, pp. 2318–2327, 2019.

[9] Y. Jiang, T. Wang, Y. Zhao, and C. Wang, "Numerical simulation of fault activation pattern induced by coal extraction," *Journal of China University of Mining & Technology*, vol. 42, no. 1, pp. 1–5, 2013.

[10] Q. Wu, P. Kong, Q. Wu et al., "Study on overburden rock movement and stress distribution characteristics under the influence of a normal fault," *Advances in Civil Engineering*, vol. 2020, Article ID 7859148, 16 pages, 2020.

[11] Z. Li, S. Bao, W. Yin, Y. Liang, and S. Sun, "Study on the activation condition of giant thrust fault under mining disturbance," *Journal of Mining & Safety Engineering*, vol. 36, no. 4, pp. 762–767, 2019.

[12] H. Jiang, J. Li, S. Deng, D. Wang, and X. Zhao, "Experimental investigation and analysis of triggering mechanism for fault-slip bursts of the tunnel surrounding rock with external disturbance," *Shock and Vibration*, vol. 2018, Article ID 1687519, 11 pages, 2018.

[13] Y. Xia, J. Wang, and D. Mao, "Analysis of fault activation induced rock burst risk based on in- situ stress measurements," *Journal of China Coal Society*, vol. 41, no. 12, pp. 3008–3015, 2016.

[14] S. Zhu, F. Jiang, K. J. A. Kouame et al., "Fault activation of fully mechanized caving face in extra-thick coal seam of deep shaft," *Chinese Journal of Rock Mechanics and Engineering*, vol. 35, no. 1, pp. 50–58, 2016.

[15] J. Jiang, Q. Wu, and H. Qu, "Characteristic of mining stress evolution and activation of the reverse fault below the hard-thick strata," *Journal of China Coal Society*, vol. 40, no. 2, pp. 267–277, 2015.

[16] J. Jiang, Q. Wu, and H. Qu, "Evolutionary characteristics of mining stress near the hard-thick overburden normal faults," *Journal of Mining & Safety Engineering*, vol. 31, no. 6, pp. 881–887, 2014.

[17] Y. Zhao, H. Wang, Z. Jiao, Z. Lu, and X. Zhang, "Experimental study of the activities of reverse fault induced by footwall coal mining," *Journal of China Coal Society*, vol. 43, no. 4, pp. 914–922, 2018.

[18] Z. Jiao, Y. Jiang, Y. Zhao, M. Zhang, and H. Hu, "Study of dynamic mechanical response characteristics of working face passing through reverse fault," *Journal of China University of Mining & Technology*, vol. 48, no. 1, pp. 54–63, 2019.

[19] H. Li, L. Zhang, Y. Weng, H. Li, and J. Yang, "Safe and high-efficient mining model in old mining area and resource integration mines," *Progress in Mine Safety Science and Engineering II*, vol. 31, no. 6, pp. 869–874, 2014.

[20] C.-P. Lu, Y. Liu, N. Zhang, T.-B. Zhao, and H.-Y. Wang, "In-situ and experimental investigations of rockburst precursor and prevention induced by fault slip," *International Journal of Rock Mechanics and Mining Sciences*, vol. 108, pp. 86–95, 2018.

[21] G. Zhu, L. Dou, H. Wang, H. Liu, and G. Dong, "Back analysis of rock burst risk and fault slip due to mining in the island panel along fault: a case study of island panel 3108 in Chaoyang coal mine," *Journal of China Coal Society*, vol. 45, no. 2, pp. 533–541, 2020.

[22] S. Zhao, Z. Deng, W. Ji et al., "Effects of multi-stage tectonic movement on regional tectonic stress characteristics and rockburst," *Journal of Mining & Safety Engineering*, vol. 36, no. 2, pp. 306–314, 2019.

[23] P. Li, M.-F. Cai, Q.-F. Guo, and S.-J. Miao, "In situ stress state of the northwest region of the jiaodong peninsula, China from overcoring stress measurements in three gold mines," *Rock Mechanics and Rock Engineering*, vol. 52, no. 11, pp. 4497–4507, 2019.

[24] Q. Zhang, C. Liu, K. Duan, Z. Zhang, and W. Xiang, "True three-dimensional geomechanical model tests for stability analysis of surrounding rock during the excavation of a deep underground laboratory," *Rock Mechanics and Rock Engineering*, vol. 53, no. 2, pp. 517–537, 2020.

[25] P. Lyu, X. Bao, G. Lyu, and X. Chen, "Research on fault activation law in deep mining face and mechanism of rockburst induced by fault activation," *Advances in Civil Engineering*, vol. 2020, Article ID 8854467, 13 pages, 2020.

[26] K. Zhang, "Mechanism study of coal bump under tectonic and ultra-thick conglomerate coupling conditions in mining roadway," *Chinese Journal of Rock Mechanics and Engineering*, vol. 36, no. 4, p. 1040, 2017.

[27] H. Wang, Y. Zhao, Z. Mu et al., "Characteristics of seismic activity and tensile-slip features of fault under stress and displacement disturbance in full-mechanized workface," *Journal of China Coal Society*, vol. 42, no. 10, pp. 2573–2581, 2017.

[28] C. Wang, F. Jiang, and J. Liu, "Analysis on control action of geologic structure on rock burst and typical cases," *Journal of China Coal Society*, vol. 37, pp. 263–268, 2012.

[29] Z. Zhu, H. Zhang, J. Han, and Y. Lv, "A risk assessment method for rockburst based on geodynamic environment," *Shock and Vibration*, vol. 2018, Article ID 2586842, 10 pages, 2018.

[30] F. Jiang, Y. Liu, M. Zhai et al., "Evaluation of rock burst hazard based on the classification of stress and surrounding rock," *Chinese Journal of Rock Mechanics and Engineering*, vol. 36, no. 5, pp. 1041–1052, 2017.

[31] A. Wang, Y. Pan, Z. Li et al., "Similar experimental study of rockburst induced by mining deep coal seam under fault action," *Rock and Soil Mechanics*, vol. 35, no. 9, pp. 2486–2492, 2014.

[32] T. Wang, S. You, and Y. Gao, "The influence of different mining modes on the evolution law of stress in fault surrounding rock," *Journal of Mining & Safety Engineering*, vol. 34, no. 2, pp. 276–281, 2017.

[33] J. Zhang, Y. Wang, Y. Sun, and G. Li, "Strength of ensemble learning in multiclass classification of rockburst intensity," *International Journal for Numerical and Analytical Methods in Geomechanics*, vol. 44, no. 13, pp. 1833–1853, 2020.

[34] B. G. Tarasov and M. F. Randolph, "Frictionless shear at great depth and other paradoxes of hard rocks," *International Journal of Rock Mechanics and Mining Sciences*, vol. 45, no. 3, pp. 316–328, 2008.

[35] F. Jiang, X. Miao, C. Wang et al., "Predicting research and practice of tectonic-controlled coal burst by microseismic monitoring," *Journal of China Coal Society*, vol. 35, no. 6, pp. 900–903, 2010.

[36] F. Meng, H. Zhou, Z. Wang et al., "Experimental study on the prediction of rockburst hazards induced by dynamic structural plane shearing in deeply buried hard rock tunnels," *International Journal of Rock Mechanics and Mining Sciences*, vol. 86, pp. 210–223, 2016.

[37] L. Jiang, P. Kong, P. Zhang et al., "Dynamic analysis of the rock burst potential of a longwall panel intersecting with a fault," *Rock Mechanics and Rock Engineering*, vol. 53, no. 4, pp. 1737–1754, 2020.

[38] L. Cong, A. Cao, Y. Zhou et al., "The comprehensive prewarning method of rock burst hazard based on theory of dynamic and static combined loading," *Journal of Mining & Safety Engineering*, vol. 37, no. 4, pp. 767–776, 2020.

[39] C. Wang, A. Cao, C. Zhang, and I. Canbulat, "A new method to assess coal burst risks using dynamic and static loading analysis," *Rock Mechanics and Rock Engineering*, vol. 53, no. 3, pp. 1113–1128, 2020.

[40] D. Li, F. Jiang, C. Wang, Z. Tian, and Y. Wang, "Study on the mechanism and prevention technology of "square position" and "stress breakdown effect" inducing rockburst," *Journal of Mining & Safety Engineering*, vol. 35, no. 5, pp. 1014–1021, 2018.

[41] F. Jiang, Y. Liu, W. Yang et al., "Relationship between rock burst and the three zone structure loading model in Yuncheng coal mine," *Journal of Mining & Safety Engineering*, vol. 34, no. 3, pp. 405–410, 2017.

[42] Y. Chen, D. Li, F. Jiang et al., "Prevention mechanism of rock burst in backfill mining in extra-thick coal seam with deep shaft," *Journal of Mining & Safety Engineering*, vol. 37, no. 5, pp. 969–976, 2020.

[43] D. Wang, Q. Wang, S. Li et al., "Stress distribution characteristics of deep mine in fully-mechanized sublevel caving face based on microseismic and online stress monitoring system," *Journal of Mining & Safety Engineering*, vol. 32, no. 3, pp. 382–388, 2015.

[44] L. Kong, Q. Qi, F. Jiang, and Z. Ouyang, "Abnormal strata stress resulted from goaf square of longwall face based on microseismic monitoring," *Chinese Journal of Rock Mechanics and Engineering*, vol. 31, pp. 3889–3896, 2012.

[45] D. Ge, D. Li, F. Jiang et al., "Reasonable pressure-relief borehole spacing in coal of different strength," *Journal of Mining & Safety Engineering*, vol. 37, no. 3, pp. 578–585, 2020.

[46] G. Su, X. Feng, Q. Jiang, and G. Chen, "Study on new index of local energy release rate for stability analysis and optimal design of underground rockmass engineering with high geostress," *Chinese Journal of Rock Mechanics and Engineering*, vol. 25, no. 12, pp. 2453–2460, 2006.